

Urea-nitrate combustion synthesis of MgO/MgAl₂O₄ nanocatalyst used in biodiesel production from sunflower oil: Influence of fuel ratio on catalytic properties and performance



Behgam Rahmani Vahid, Mohammad Haghighi *

Chemical Engineering Faculty, Sahand University of Technology, P.O. Box 51335-1996, Sahand New Town, Tabriz, Iran

Reactor and Catalysis Research Center (RCRC), Sahand University of Technology, P.O. Box 51335-1996, Sahand New Town, Tabriz, Iran

ARTICLE INFO

Article history:

Received 12 May 2016

Received in revised form 16 July 2016

Accepted 18 July 2016

Keywords:

MgO/MgAl₂O₄

Nanocatalyst

Urea-nitrate combustion synthesis

Biodiesel

Sunflower oil

ABSTRACT

MgO/MgAl₂O₄ nanocatalyst was synthesized by a simple, cost-effective and rapid method and used in biodiesel production from sunflower oil. MgAl₂O₄ was synthesized by combustion method at different fuel ratios and then active phase of MgO was dispersed on the samples by impregnation method. The nanocatalysts were characterized by XRD, FESEM, EDX, BET-BJH, TGA and FTIR analyses, so as to optimize the concentration of urea (as fuel) in the combustion synthesis. The physicochemical properties of the nanocatalyst confirmed the sample synthesized with fuel ratio of 1.5 has high surface area, effective morphology and texture properties. Finally, in order to evaluate catalytic activity of the samples in biodiesel production, the transesterification reaction was performed. The results indicated the catalyst prepared by combustion synthesis with a fuel ratio of 1.5 was optimum specifications for biodiesel production. Using this catalyst, 95% of sunflower oil was successfully converted to biodiesel. Furthermore, the optimal catalyst showed relatively good reusability, making it a good choice for industrial biodiesel production.

© 2016 Published by Elsevier Ltd.

1. Introduction

Nowadays, for reasons such as concerns about greenhouse gases, diminishing fossil fuel and crude oil resources, and soaring global energy demands [1,2], researchers are well encouraged to develop alternative, renewable and nontoxic fuels [3–5]. Biodiesel has attracted many researchers because of its combustion properties that are similar to those of fossil diesel [6–8]. Fatty acid methyl esters (FAME) are produced by transesterification of triglycerides with methanol or esterification of free fatty acids (FFAs) with methanol. Biodiesel is produced using either of homogeneous or heterogeneous catalysts [9–11]. Although homogeneous catalysts have several advantages such as high catalytic activity and mild reaction conditions [12,13], the use of them is associated with several problems including soap formation [14]. Unlike homogeneous catalysts, heterogeneous variants are recyclable, i.e. they can be reused several times, leading to better separation of the final product [15–17]. However, heterogeneous catalysts can address associated problems with homogeneous catalysts [18–20].

* Corresponding author at: Reactor and Catalysis Research Center, Sahand University of Technology, P.O. Box 51335-1996, Sahand New Town, Tabriz, Iran.

E-mail address: haghighi@sut.ac.ir (M. Haghighi).

URL: <http://rcrc.sut.ac.ir> (M. Haghighi).

<http://dx.doi.org/10.1016/j.enconman.2016.07.050>
0196-8904/© 2016 Published by Elsevier Ltd.

Heterogeneous solid acid catalysts such as SO₄²⁻/ZnO [17], SO₃H-ZnAl₂O₄ [21], WO₃/ZrO₂ [22] and Zr-MOFs [23] can be used in both transesterification and esterification reactions [24]. However, for complete conversion to biodiesel, acid catalysts require high alcohol-to-oil molar ratios, high catalyst concentrations, and longer reaction times to achieve satisfactory transesterification conversions [14,17]. Even though the performances of solid acid catalysts are still inferior compared to the solid base catalysts when it comes to transesterification reaction [1], they are still suitable for esterification reaction. For this reason, a variety of heterogeneous solid base catalysts have been examined for biodiesel synthesis, mostly in transesterification reaction. CaO-ZrO₂ [1], Mg-Al [25–28], Na₂O/NaX [16] and MgAl₂O₄ spinel [29] are some of traditional heterogeneous solid base catalysts that have been used in transesterification reaction. Spinel is an important class of oxide materials which have many potential catalytic applications [29–31]. Among other advantages and properties of spinels, one can refer to insignificant deactivation of catalysts by leaching in spinel-involved processes [5] and substitution of large percentages of one or both of the spinel components with other groups with no modification of the crystal structure [32]. Studied as a catalyst or catalyst support in chemicals production [33–35], magnesium aluminium spinel (MgAl₂O₄) has been successfully used in methanolysis of soybean oil [29].

The physicochemical properties and catalytic performance of a synthesized nanocatalyst could be affected by synthesis method [36–38]. In the present study, magnesium aluminium spinel was prepared via combustion method which has the advantage of being quick and easy synthesis method, as well as enlarged pores formation in the catalyst. These benefits make this catalyst an economic one for the reaction of biodiesel production that the solution in the reaction comprises large molecules of triglycerides. $MgAl_2O_4$ spinel, due to its distinguished properties such as thermal resistance, high surface area and porosity is very practical, especially for biodiesel production which was synthesized by the combustion method and for the first time used for biodiesel reaction in this study. The synthesized $MgAl_2O_4$ spinel was then used as a heterogeneous catalyst support on which MgO (as the active phase) was deposited before further testing the resultant catalyst in transesterification reactions. Effect of fuel ratio on combustion synthesis was investigated to find an optimal catalyst.

2. Materials and methods

2.1. Materials

For the synthesis of nanostructured $MgO/MgAl_2O_4$ catalysts using combustion method, magnesium nitrate ($Mg(NO_3)_2 \cdot 6H_2O$; Merck, 99%), aluminium nitrate ($Al(NO_3)_3 \cdot 9H_2O$; Merck, 99%) and urea (NH_2CONH_2 ; Romil, 99.5%) were used without further purifi-

cation. For the production of biodiesel, sunflower oil (acid content <0.3 mg KOH/g) and methanol (Merck, 99.9%) were used as reactants of transesterification.

2.2. Nanocatalysts preparation and procedure

A schematic flowchart of the steps involved in the synthesis of $MgO/MgAl_2O_4$ nanocatalysts is represented in Fig. 1. As shown in the figure, in the first step, $MgAl_2O_4$ was prepared by a simple solution combustion method. For the synthesis of 4 g of $MgAl_2O_4$, at first, approximately 29 mmol of $Mg(NO_3)_2 \cdot 6H_2O$ along with 57 mmol $Al(NO_3)_3 \cdot 9H_2O$ were dissolved into 70 ml of deionized water. After 20 min of mixing the solution, various molar ratios of urea (0.5–2 times of the stoichiometric ratio) were added to the solution. The mixture was heated to 70 °C and then stirred with a magnet stirrer for about 3 h until a transparent gel was obtained. The gel was placed in an electric furnace at 350 °C where it released white smoke (i.e. combustion started) in a few minutes, with the time to start the combustion process depending on the fuel ratio in the mixture. After the reaction, the obtained low-density white foam was crushed in a ceramic mortar. In the second step, the $MgO/MgAl_2O_4$ nanocatalysts were prepared by the impregnation method using an aqueous solution of $Mg(NO_3)_2 \cdot 6H_2O$. For all of the samples, 10 wt.% MgO was loaded on the support ($MgAl_2O_4$); for this purpose, a solution was prepared considering

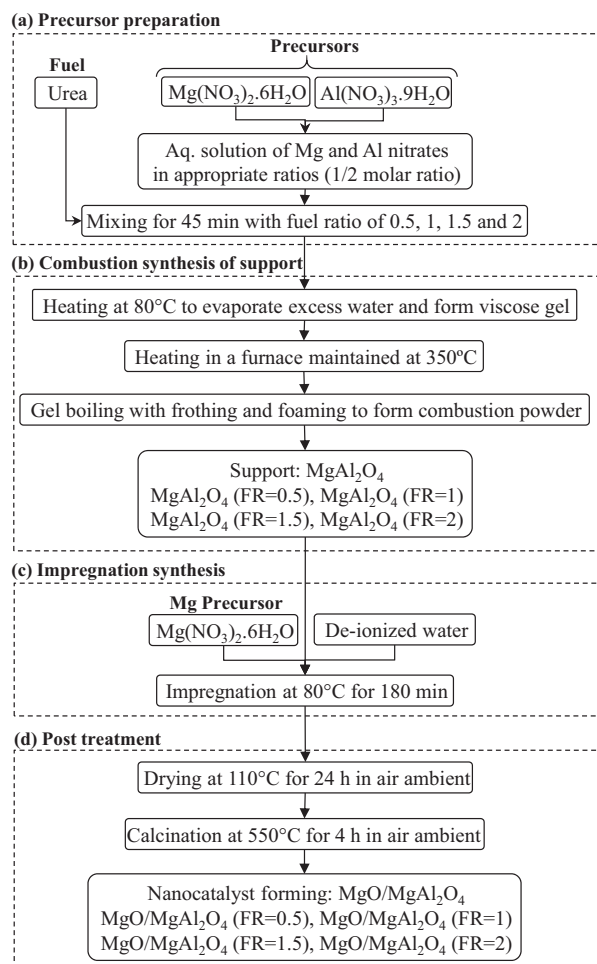


Fig. 1. Urea-nitrate combustion synthesis of $MgO/MgAl_2O_4$ nanocatalyst with various fuel ratios.

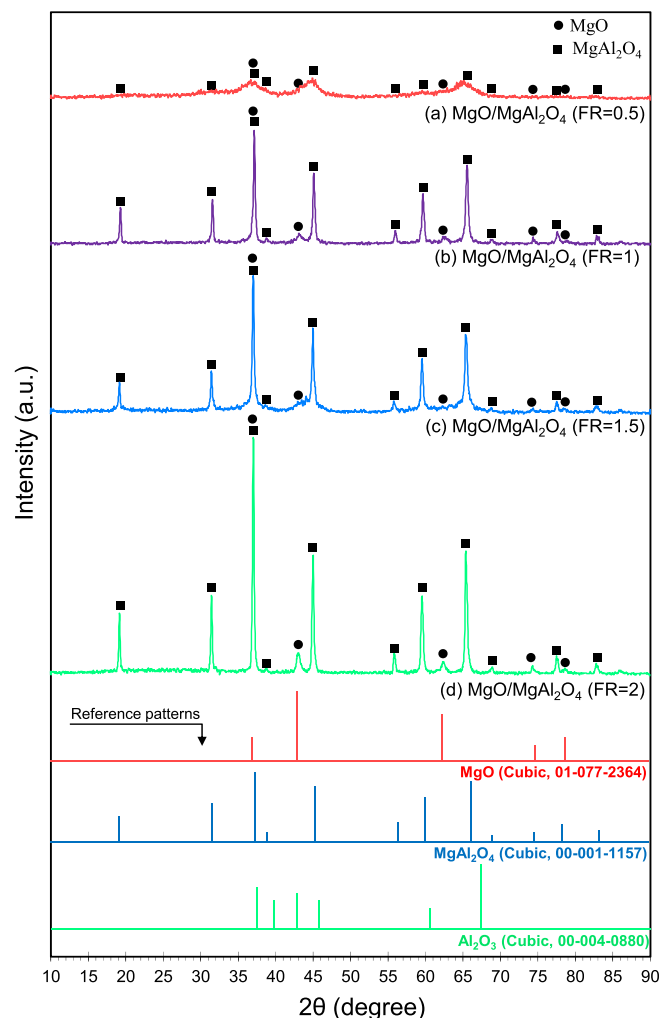


Fig. 2. XRD patterns of synthesized $MgO/MgAl_2O_4$ nanocatalysts with various fuel ratios: (a) FR = 0.5, (b) FR = 1, (c) FR = 1.5 and (d) FR = 2.

the required amount of magnesium nitrate hexahydrate. Then, the support was added to the solution and the mixture was stirred on a magnet stirrer while heated at 70 °C for 4 h. Thereupon, the mixture was dried at 110 °C for 24 h before being calcined at 550 °C for 4 h.

2.3. Nanocatalysts characterization techniques

The synthesized samples were characterized by XRD, FESEM, EDX, TGA, BET-BJH and FTIR techniques. In order to study crystallographic properties of the nanocatalysts, they were subject to XRD analysis on a D-5000 diffractometer (Germany, Siemens, Cu K α radiation, 0.154056 nm) operated in the range of $2\theta = 10\text{--}90^\circ$. Surface morphologies of the samples were investigated by a FESEM (Field Emission Scanning Electron Microscopy) on MIRA3 FEG-SEM (Czech Republic, TESCAN) analyser. For surface compositional analysis, EDX-Dot mapping analysis was performed by a VEGA II Detector (Czech Republic, TESCAN). TGA analysis was used to detect incomplete decomposition of nitrate and urea (as the fuel) during the combustion synthesis. The TGA analysis was performed using a Perkin Elmer Pyris Diamond apparatus in which a flow of air was provided; the air was heated from 50 to 600 °C at a heating rate of 10 °C min⁻¹. In an attempt to determine surface area of the nanocatalysts, X Quanta chrome chembet-3000 was used for BET analysis. Furthermore, BJH method (Barrett-Joyner-Halenda) was utilized to obtain relative pore size and volume in a wide range of pore size distributions. Using FTIR technique, infrared spectrum of absorption/desorption of the samples were captured by a TENSOR 27 (Germany, Bruker) which was operated in the range of 400–4000 cm⁻¹ via K-Br pellet method.

2.4. Experimental setup for catalytic performance test

A stainless-steel reactor with an internal Teflon container of 100 cm³ capacity was used for the transesterification reaction. The reactor was covered by a controllable heater clamp which was placed on a magnetic stirrer. All the reactions were performed under the same conditions: reaction temperature = 110 °C, reaction time = 3 h, methanol-to-oil molar ratio = 12, and catalyst concentration = 3 wt.%; the conditions were adopted from other works done to find an optimal catalyst for similar situations, as well as criteria for evaluating optimal sample with similar catalysts [26–28]. The products of transesterification (FAMES) were analysed by a gas chromatograph (GC Chrom, Teif Gostar Faraz, Iran). The GC was equipped with a FID (Flame Ionization Detector) and a SUPRAWAX-280 column (Spain, Teknokroma). Injection was done in split mode (1/100) with the injector and detector adjusted at 260 °C. Samples (1 μ l) were

injected and hydrogen was used as the carrier gas by inlet pressure of 14 psi for the analysis. To ensure accuracy of the results, the tests were undertaken in triplicate.

3. Results and discussions

3.1. Nanocatalysts characterization

3.1.1. XRD analysis

Fig. 2 shows the corresponding XRD patterns to MgO/MgAl₂O₄ samples prepared by combustion synthesis method with four different fuel ratios. Comparing the diffraction peaks with reference patterns, it was clearly observed that the peaks at $2\theta = 19.2, 31.6, 37.3, 45.3, 60.0$ and 66.2 (JCPDS: 00-001-1157) were related to cubic phase of MgAl₂O₄ and the peaks at $2\theta = 37.0, 43.0, 62.4, 74.8$ and 78.7 (JCPDS: 01-077-2364) were attributed to cubic phase of MgO, indicating successful formation of the crystals. It is worth noting that comparison of XRD patterns showed no similarity between the synthesized nanocatalysts and hydrocalcite phase (JCPDS No 00-022-0700) which has its main peaks at $2\theta = 11.2, 22.8, 34.5, 38.6, 45.5, 46.5, 60, 61.9$ and 65.8 . Therefore, no hydrocalcite formation can be detected in fabricated samples. According to the corresponding reference pattern to alumina (JCPDS: 00-004-0880), alumina was not observed in the synthesized nanocatalysts. As shown in Table 1, relative crystallinity of samples synthesized with fuel ratios of 0.5, 1, 1.5 and 2 were found to be 5, 30, 55 and 100, respectively, showing the enhancement of the crystallinity by increasing the fuel ratio. Moreover, calculated by Scherrer equation [39], the crystallite size of samples exhibited similar behaviour to those of relative crystallinity.

3.1.2. FESEM analysis

Fig. 3 shows the surface morphology of the synthesized catalysts (MgO/MgAl₂O₄) with different fuel ratios, as captured by FESEM analysis. In Fig. 3(a–d), it is clear that, pore diameters increase by increasing the fuel ratio from 0.5 to 2. This is due to increased combustion exhausts emitted within a very short period of time [40,41]. Particles of the catalyst prepared with a fuel ratio of 0.5 (Fig. 3(a)) were smaller than those of the other catalysts, probably due to the lack of crystal growth in the absence of sufficient heat of combustion, as discussed in the section on XRD analysis. Also, such tiny particles were likely to increase surface area, as mentioned in the section on BET analysis. Although particle agglomeration was observed in all cases, the agglomerations were different in their pore structures. Fig. 3(c) and (d) shows the synthesized samples with fuel ratios of 1.5 and 2; the samples exhibit a honeycomb structure with relatively large pore diameters, which is in agreement with the BET analysis results. Accordingly, these

Table 1
Structural properties of synthesized MgO/MgAl₂O₄ nanocatalyst.

Nanocatalyst	MgO (wt.%)	MgAl ₂ O ₄ (wt.%)	Fuel ratio (to stoichiometric)	Surface area (m ² /g)	Pore volume (cm ³ /g)	Mean pore size (nm)	Relative crystallinity ^a		Crystallite size ^b (nm)	
							MgAl ₂ O ₄	MgO ^c	MgAl ₂ O ₄ ^d	
MgO/MgAl ₂ O ₄ (FR = 0.5)	10	90	0.5	136.8	0.1794	5.6	5.5	–	–	
MgO/MgAl ₂ O ₄ (FR = 1)	10	90	1	43.3	0.0445	4.3	46.1	12.6	29.2	
MgO/MgAl ₂ O ₄ (FR = 1.5)	10	90	1.5	60.6	0.0787	6.3	55.8	–	30.6	
MgO/MgAl ₂ O ₄ (FR = 2)	10	90	2	57.7	0.0691	5.8	100	16.5	33.5	

^a Relative crystallinity: XRD relative peak intensity.

^b Crystallite size estimated by Scherrer's equation.

^c Crystallite phase: Cubic (JCPDS: 01-077-2364, $2\theta = 37.0, 43.0, 62.4, 74.8$ and 78.7).

^d Crystallite phase: Cubic (JCPDS: 00-001-1157, $2\theta = 19.2, 31.6, 37.3, 45.3, 60.0$ and 66.2).

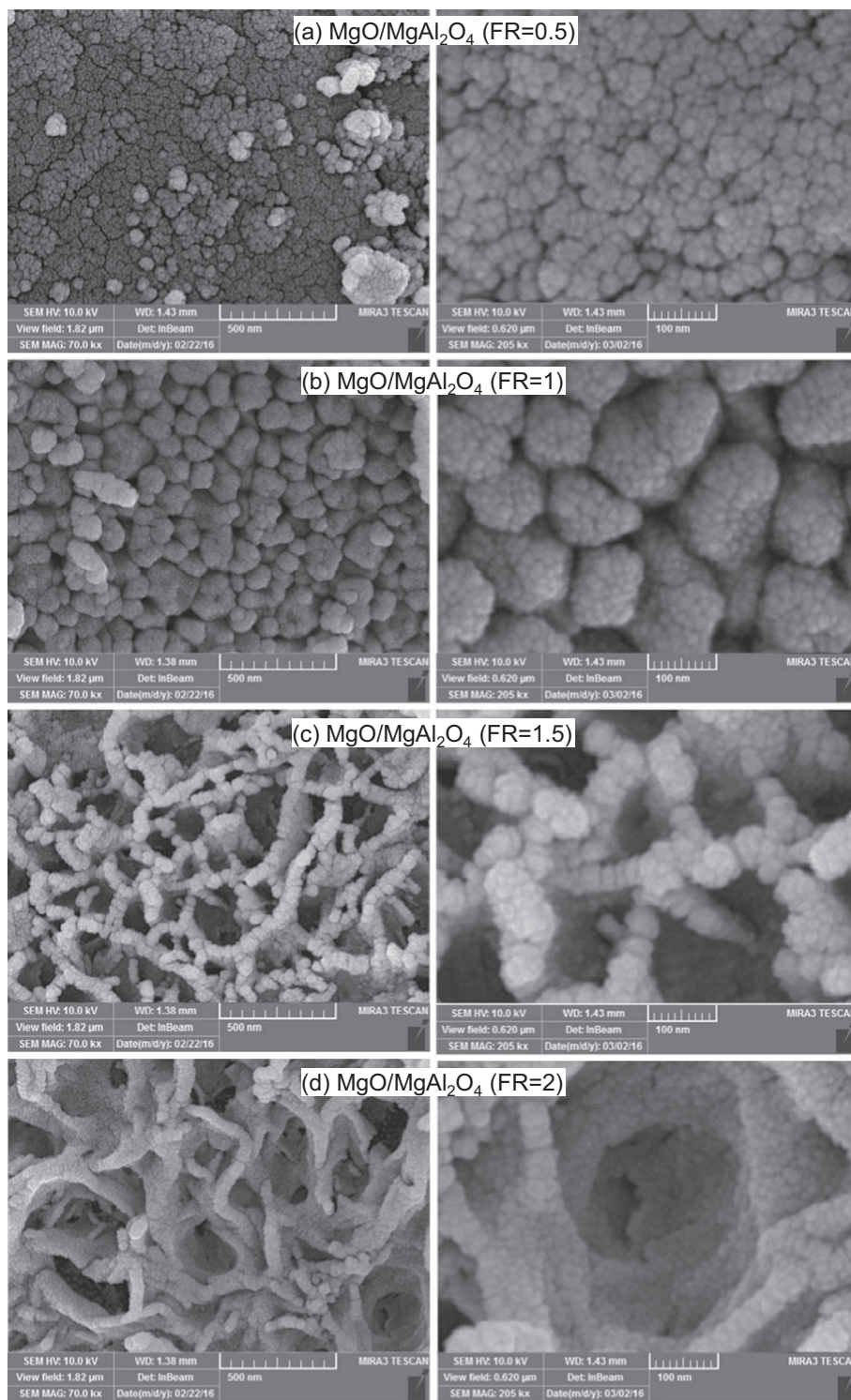


Fig. 3. FESEM images of synthesized $\text{MgO/MgAl}_2\text{O}_4$ nanocatalysts with various fuel ratios: (a) FR = 0.5, (b) FR = 1, (c) FR = 1.5 and (d) FR = 2.

catalysts seem to be more appropriate for biodiesel production [42,43]. Fig. 4 indicates the distribution of surface particle sizes [44] for the synthesized catalyst with a fuel ratio of 1.5. Minimum and maximum particle sizes were 6.8 and 30.9 nm, respectively, with an average size of 15.9 nm. For all crystal sizes, the results were consistent with the results of XRD analysis. In addition, the analysis showed the appropriate distribution of particles in the range of 10–20 nm.

3.1.3. EDX analysis

The results of EDX analysis of $\text{MgO/MgAl}_2\text{O}_4$ samples synthesized with different fuel ratios (from 0.5 to 2) are shown in Fig. 5. It can be seen from the EDX analysis results that, Al, Mg, and O elements exhibited proper distributions with no agglomerated particles – very important parameters when it comes to catalytic activity [45]. The results further revealed that, at the end of the catalyst synthesis process, no impurities (including fuel (car-

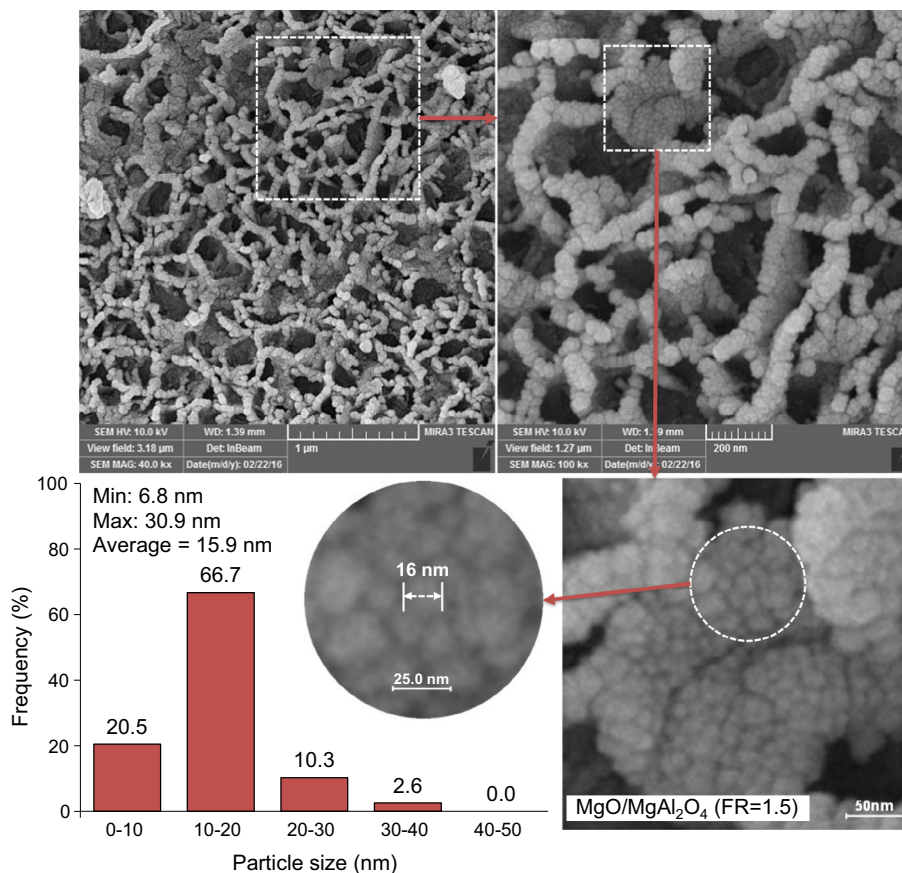


Fig. 4. Surface particle size distribution histogram of synthesized nanocatalyst: MgO/MgAl₂O₄ (FR = 1.5).

bon) and nitrate precursors (nitrogen)) remained. Fig. 6 shows the percentages of the Al, Mg and O elements, as obtained by EDX analysis of the synthesized catalysts, along with the corresponding original percentages in the initial gel. Considering the original percentages, the obtained percentages of the elements in all of the synthesized catalysts were acceptable.

3.1.4. TGA analysis

Fig. 7 shows TGA analysis of the synthesized samples with different fuel ratios. The analysis was used for the detection of residual fuel from the combustion and residual nitrate precursors. For all samples, a large loss of weight was observed at temperatures from 100 to 250 °C; the loss was attributed to the evaporation and removal of physically adsorbed water. The slight loss of weight (less than 1%) at temperatures from 250 to 400 °C was corresponded to the decomposition of magnesium and aluminium nitrates. Such a small loss of weight within this temperature region indicated a suitable precursor decomposition during the combustion synthesis, so that an insignificant weight loss was observed for all samples except for the MgO/MgAl₂O₄ (FR = 0.5) when heated to higher than 400 °C. The reduction in this temperature region was due to the elimination of remaining urea in the sample because of low combustion temperature during the synthesis of the MgO/MgAl₂O₄ (FR = 0.5) catalyst.

3.1.5. BET analysis

The specific surface area, total pore volume and mean pore diameter of the prepared nanocatalysts using different fuel ratios were calculated from the isotherm data and are listed in Table 1 with their adsorption/desorption isotherms depicted in Fig. 8. As specified in the table, the sample synthesized with a fuel ratio of

0.5 showed the largest surface area and pore volume due to incomplete combustion; It should be noted that lower fuel amount of the sample with fuel ratio of 0.5 led to insufficient heat of reaction and incomplete decomposition of Mg and Al precursors. Therefore, the amorphous phase of these materials formed (according to the XRD analysis). Thus, the formed particles in this sample were smaller than crystallized samples which means they possessed higher surface area, and this surface area is an exception. However, this parameter increased by increasing the fuel ratio for other samples. It could be because of better combustion process during catalyst synthesis and large volume of the combustion exhaust. By increasing of the fuel ratio to 1, the heat of combustion increased to a sufficient amount which lead to better and complete decomposition of precursors than previous sample (fuel ratio 0.5) and cause formation of MgAl₂O₄ crystals. Moreover, by increasing of this ratio to 1.5, the heat of combustion and also exhaust gases increased more than before which amended the synthesis process condition and cause far higher surface area. Ultimately, by changing this ratio to 2, according to highest heat of combustion and exhaust gases, the crystals size extremely increased, so, as a result, there is a decline in surface area. Mean pore diameter over all samples was obtained to be over 2 nm by the BJH method, proving all catalysts to be mesoporous. Also, according to Fig. 9, a major portion of pore diameter distribution is concentrated in the range of 4–7 nm for all catalysts. There are reports indicating that, mesoporous catalysts with pore diameters of larger than 3.5 nm are appropriate for biodiesel production [42,43]. Therefore, compared to other samples, the samples prepared with fuel ratios of 1.5 and 2 were expected to convert larger amounts of triglycerides to ester. In addition, as shown in Fig. 8, the corresponding isotherms to all samples were classified as type IV and type H1 isotherm hysteresis loops, indicat-

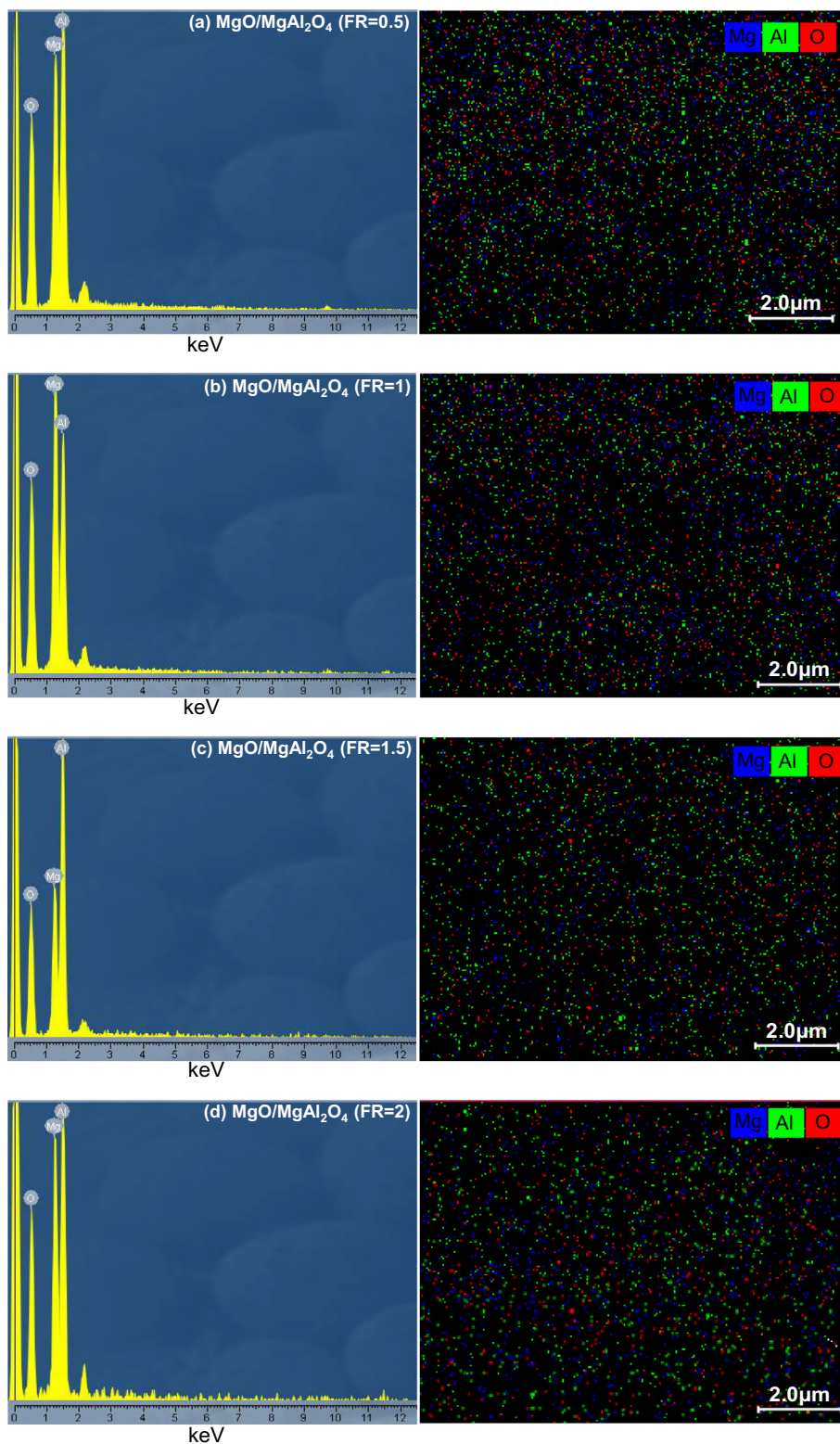


Fig. 5. EDX analysis of synthesized $\text{MgO/MgAl}_2\text{O}_4$ nanocatalysts with various fuel ratios: (a) FR = 0.5, (b) FR = 1, (c) FR = 1.5 and (d) FR = 2.

ing the pores to be of cylindrical form – seemingly an appropriate structure for the entry of large oil molecules.

3.1.6. FTIR analysis

FTIR spectra of the prepared supports (MgAl_2O_4) using various fuel ratios were captured in the range of $400\text{--}4000\text{ cm}^{-1}$ and illus-

trated in Fig. 10. The broad bands at around 1640 and 3489 cm^{-1} attributed to O–H stretching and bending modes of the water adsorbed by the surface of MgAl_2O_4 , respectively [46–48]. The peaks at around 2924 and 2856 cm^{-1} appointed to C–H stretching vibrations coming from un-combusted urea during the synthesis [49,50]. The peaks appearing at 878 , 1387 and 1514 cm^{-1} related

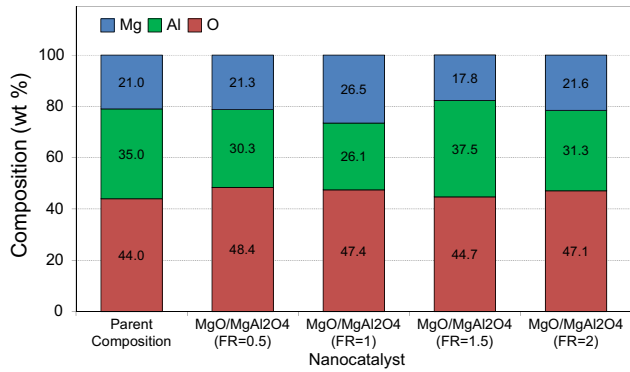


Fig. 6. Parent solution vs. surface chemical analysis of synthesized MgO/MgAl₂O₄ nanocatalysts with various fuel ratios.

to the vibration of NO₃⁻ groups [41,50,51]. As specified in the figure, for the prepared sample with a fuel ratio of 0.5, the peaks are sharper than those of other samples, proving incomplete combustion and lack of heat for the decomposition of the nitrate precursors. The strong absorption peaks within the range of 400–800 cm⁻¹ (469, 518 and 699 cm⁻¹) for the samples synthesized with fuel ratios of 1, 1.5 and 2 could be corresponded to the [AlO₆] groups and the lattice vibration of Mg–O stretching. These indicated the

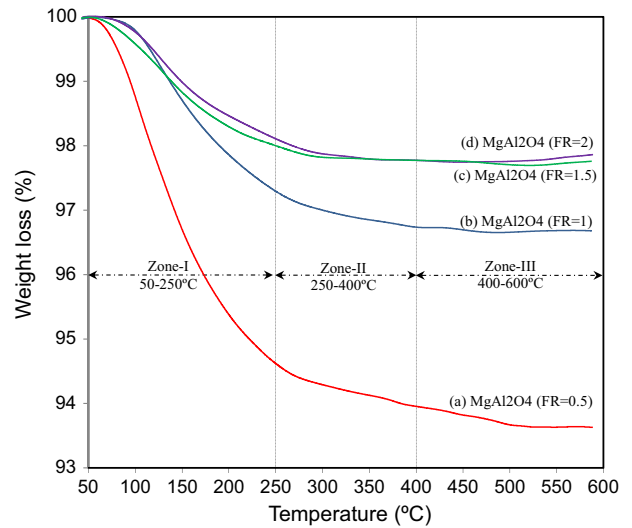


Fig. 7. TG analysis of synthesized MgAl₂O₄ supports with various fuel ratios: (a) FR = 0.5, (b) FR = 1, (c) FR = 1.5 and (d) FR = 2.

formation of MgAl₂O₄ spinel in the samples [41,49,52,53]. The defect or absence of these bands in the sample synthesized with a fuel ratio of 0.5 shows its low crystallinity [41].

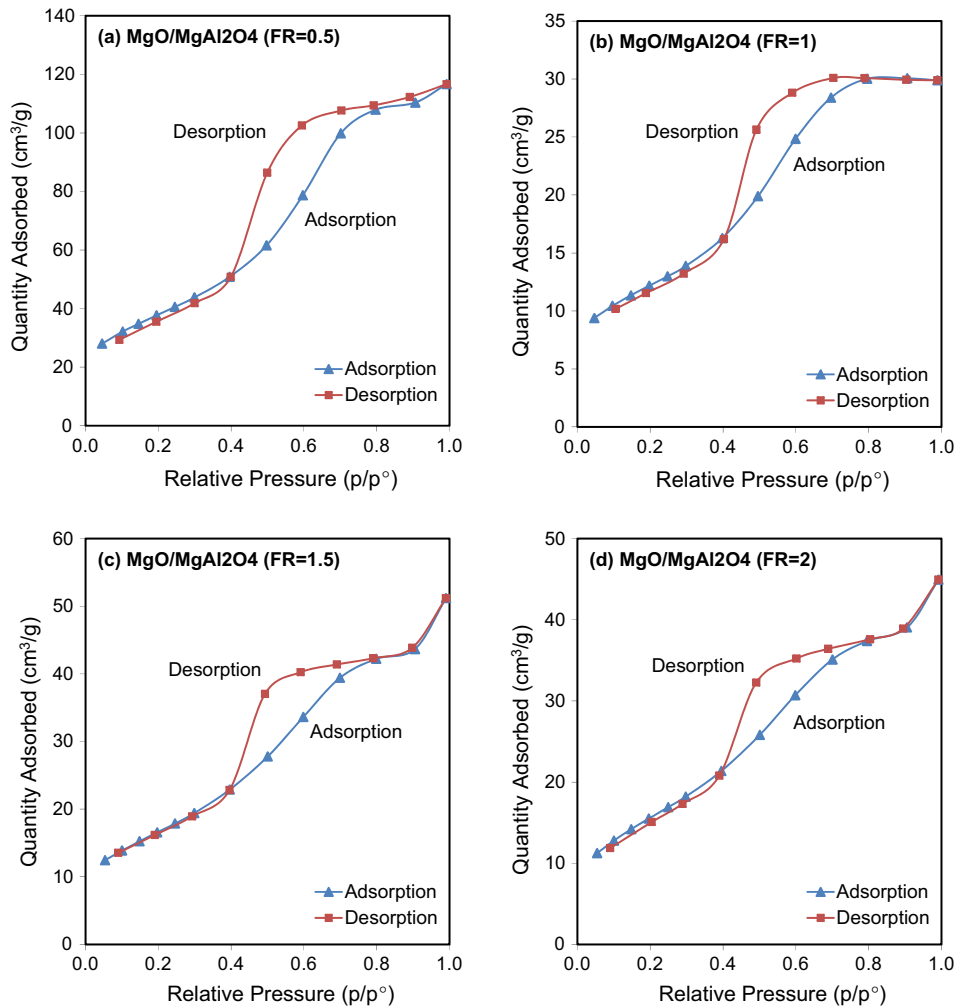


Fig. 8. Adsorption/desorption isotherms of synthesized MgO/MgAl₂O₄ nanocatalysts with various fuel ratios: (a) FR = 0.5, (b) FR = 1, (c) FR = 1.5 and (d) FR = 2.

3.2. Study of catalytic performance in biodiesel production

Continuing with the research, performance of the prepared nanocatalysts in biodiesel production was studied under the same reaction conditions (reaction temperature = 110 °C, reaction time = 3 h, methanol-to-oil molar ratio = 12, and catalyst concentration = 3 wt.%). Transesterification of sunflower oil was performed by the four prepared samples with different fuel ratios. The conversion of produced biodiesel was obtained by GC analysis (Fig. 11). As seen in the figure, the conversion increased by increasing the fuel ratio, so that the difference between the corresponding conversions to the synthesized catalysts with fuel ratios of 0.5 and 1 was found to be about 50%. This difference is probably due to incomplete formation of crystals in the MgO/MgAl₂O₄ (FR = 0.5), as explained in the section on XRD analysis. The difference between the corresponding conversions to the prepared MgO/MgAl₂O₄ samples with fuel ratios of 1 and 1.5 was as low as about 15%. This difference is likely due to increased pore diameter and surface area [43]. As can be seen in Fig. 11, by increasing the fuel ratio from 1.5 to 2 in the synthesized samples, no significant change is seen in the conversion (95.7 and 94.8%, respectively). According to Table 1, average pore diameters and surface areas of MgO/MgAl₂O₄ (FR = 1.5) and MgO/MgAl₂O₄ (FR = 2) are almost identical, proving the important role played by pore diameter in the transesterification reaction.

To sum up, a fuel ratio of 1.5 can be considered as the optimal ratio for the synthesis of the catalyst. Accordingly, the MgO/MgAl₂O₄

(FR = 1.5) sample was selected and compared with similar catalysts. In Table 2, a number of similar catalysts in the literature are compared against the optimal catalyst in the present work, with the biodiesel reaction conditions included. Although the reaction conditions used in this work are milder than those of other works, higher conversion were obtained in the current work; this might be due to suitable structure of the optimal catalyst with enlarged pores. Also our study have more advantages than the researches which were reported in the literature such as using lower MgO amount as active phase in synthesized catalyst, far simpler and swifter synthesis method (combustion method) that will help us diminish catalyst preparation time and improving the process conditions. In total, the mentioned features make the prepared catalyst an appropriate alternative for biodiesel production process, which can contribute to the economy of the process considering the required mild reaction conditions.

3.3. Reusability

Reusability represents one of the most important features of the catalysts to be used in the process of biodiesel production. Hereupon, reusability of the optimal catalyst was evaluated under the reaction conditions. Following each reaction, the used catalyst was separated from the products and washed for several times with methanol before being placed in an oven at 110 °C for 24 h after which time it was ready to be reused for the next run of the transesterification reaction. The results of the reusability of

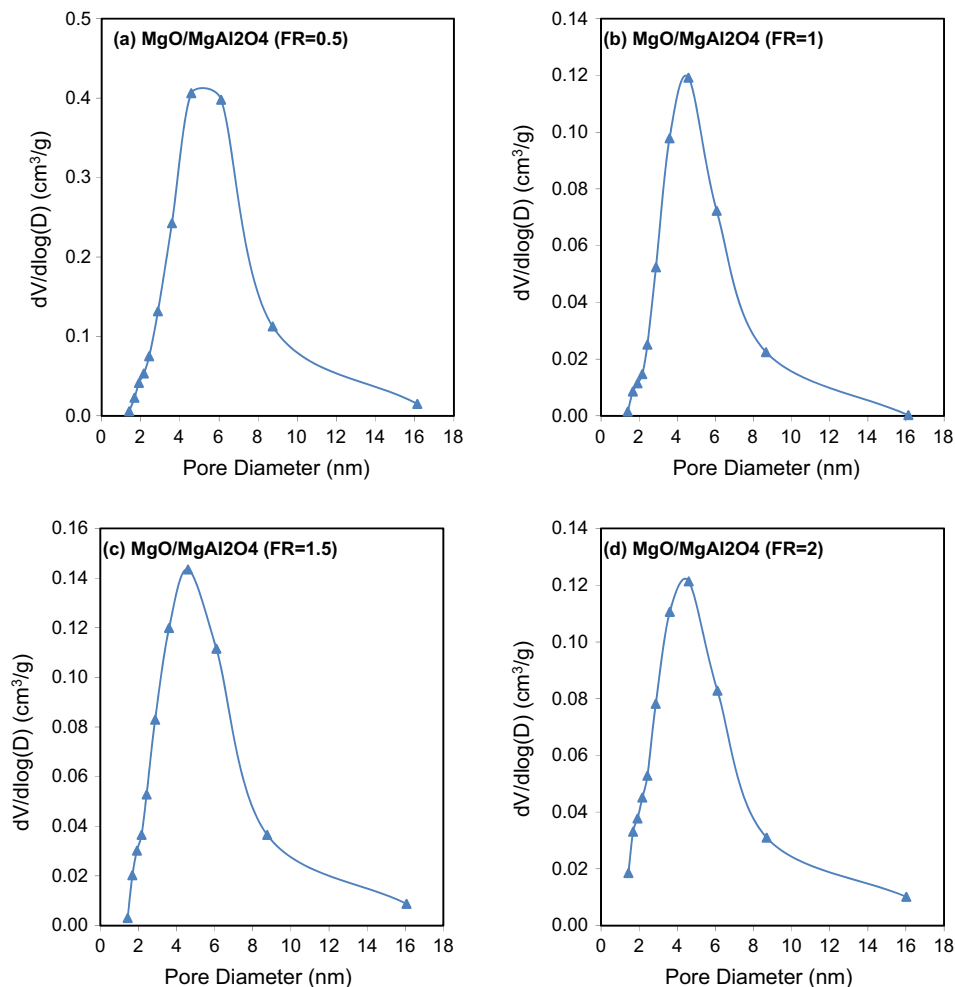


Fig. 9. Pore size distribution of synthesized MgO/MgAl₂O₄ nanocatalysts with various fuel ratios: (a) FR = 0.5, (b) FR = 1, (c) FR = 1.5 and (d) FR = 2.

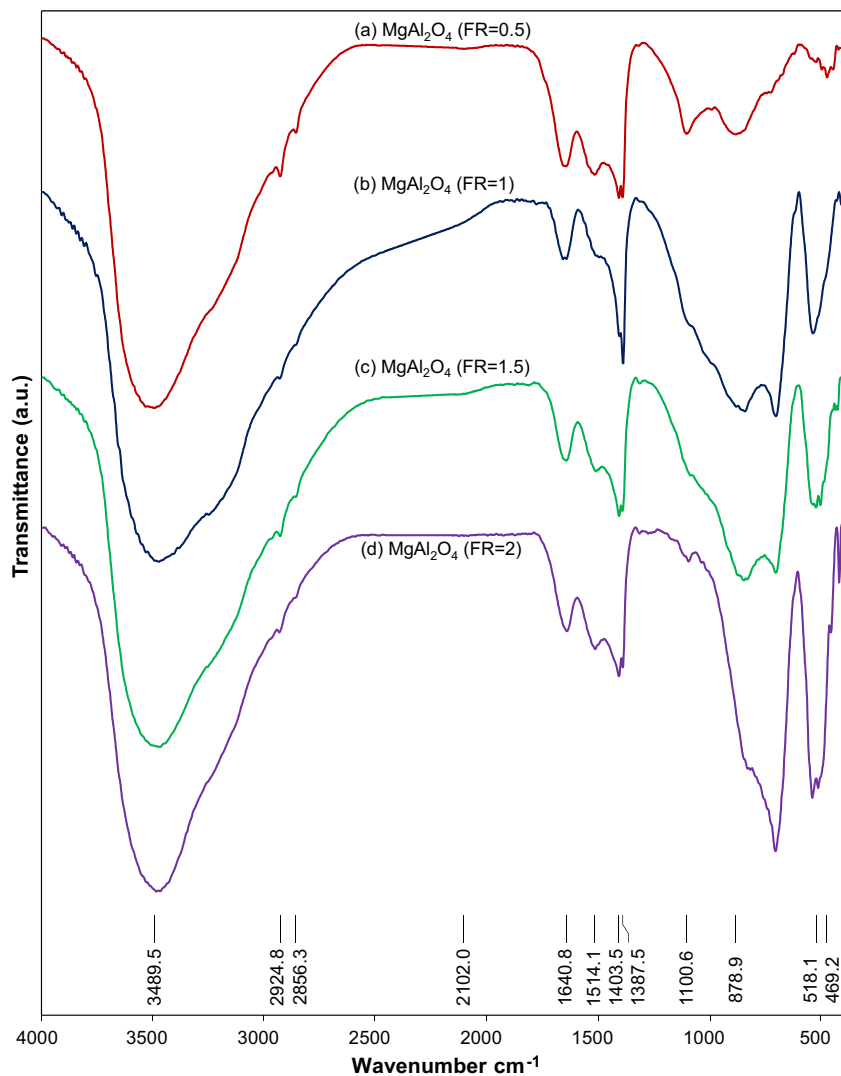


Fig. 10. FTIR spectra of synthesized MgAl_2O_4 supports with various fuel ratios: (a) FR = 0.5, (b) FR = 1, (c) FR = 1.5 and (d) FR = 2.

the optimal catalyst are shown in Fig. 12. Based on the results, the optimal catalyst showed about 5% and 9% reductions in conversion at the second and third runs of the reaction, respectively (91% and

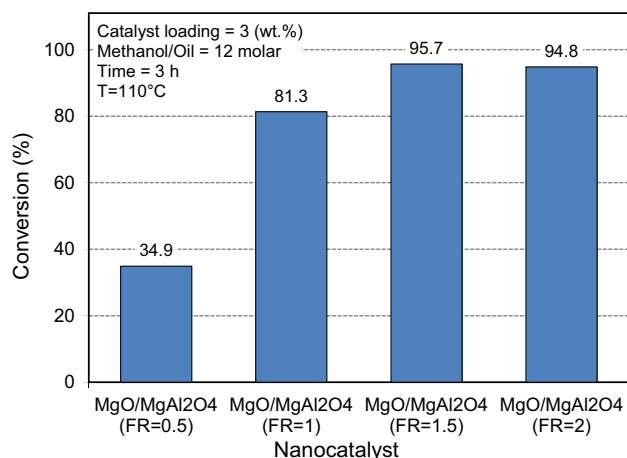


Fig. 11. Influence of fuel ratio on catalytic performance of synthesized $\text{MgO}/\text{MgAl}_2\text{O}_4$ nanocatalysts with various fuel ratios.

81.9%, respectively). In the fourth to sixth runs, no significant change in the conversion was observed compared to the third run. The reduction in the conversion can cause some leaching of the active phase (MgO) from the support (MgAl_2O_4) [2,13,54]. During the first run a small amount of MgO as active phase, which were not strongly fastened to MgAl_2O_4 surface, were readily leached into the reaction solution and this reduction in active phase amount on the support surface was a reason for diminished conversion until run 3. From run 3 onwards, the remained active phase on support material failed to leach easily to the reaction solution than previous runs (run 1 and 2). Accordingly, following the third run, no more leaching of the active phase has taken place, leaving the conversion unchanged.

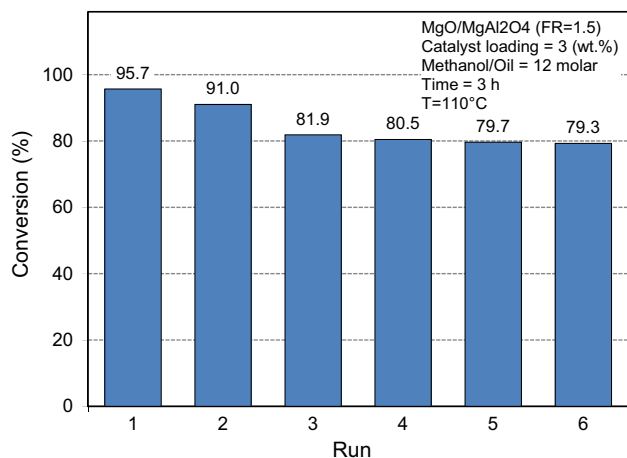
4. Conclusions

As a base catalyst for biodiesel production, MgAl_2O_4 spinel was successfully synthesized by combustion method with MgO (as the active phase) deposited on the catalyst surface. Analysing the effect of fuel ratio on the combustion synthesis of MgAl_2O_4 , it was revealed that, the synthesized base catalyst with a fuel ratio of 1.5 was of the best specifications for biodiesel production process. The optimal catalyst had an average pore diameter and surface

Table 2

Reaction condition comparison and catalytic performance of different Mg-Al mixed oxide catalysts appraised for the biodiesel production.

Catalyst	Reaction condition				Biodiesel yield (Y) or conversion (X) %	Reference
	Temperature (°C)	MeOH:Oil molar ratio	Amount of catalyst (% wt/wt)	Time (h)		
Mg-Al mixed oxide	140	24:1	–	1.54	Y = 77	[55]
Mg-Al mixed oxide	117	24:1	4	8	Y = 78	[26,28]
Mg-Al mixed oxide	115	14:1	4	2	X = 95.4	[27]
Mg-Al mixed oxide	160	12:1	6	6	Y = 90	[25]
Mg-Al-CO ₃ mixed oxide	200	6:1	1	3	X = 99	[56]
Al/(Mg + Al) mixed oxide	230	13:1	5	1	X = 90	[54]
MgO/MgAl ₂ O ₄	110	12:1	3	3	X = 95.7	This work

**Fig. 12.** Reusability of MgO/MgAl₂O₄ (FR = 1.5) nanocatalyst toward biodiesel production from sunflower oil.

area of 6.3 nm and 60.6 m²/g, respectively; indeed, the specifications are much suitable for biodiesel production process. The optimum catalyst showed superior efficiency (95.7%) along with slight loss of reusability compared to other similar catalysts studied in related literatures under the same reaction conditions. Successfully used in biodiesel production reaction, the prepared optimal MgO/MgAl₂O₄ catalyst represented an efficient and cost-effective catalyst which can be readily synthesized. Future researches may investigate the catalyst reusability and mild reaction conditions, so as to achieve more economical production of biodiesel.

Acknowledgements

The authors gratefully acknowledge Sahand University of Technology for the financial support of the research as well as Iran Nanotechnology Initiative Council for complementary financial supports.

References

- Xia S, Guo X, Mao D, Shi Z, Wu G, Lu G. Biodiesel synthesis over the CaO-ZrO₂ solid base catalyst prepared by a urea-nitrate combustion method. *RSC Adv* 2014;4:51688–95.
- Zabeti M, Daud WMAW, Aroua MK. Biodiesel production using alumina-supported calcium oxide: an optimization study. *Fuel Process Technol* 2010;91:243–8.
- Ma C, Yu J, Wang B, Song Z, Xiang J, Hu S, et al. Chemical recycling of brominated flame retarded plastics from e-waste for clean fuels production: a review. *Renew Sustain Energy Rev* 2016;61:433–50.
- Azami MH, Savill M. Modelling of spray evaporation and penetration for alternative fuels. *Fuel* 2016;180:514–20.
- Mierczynski P, Ciesielski R, Kedziora A, Maniukiewicz W, Shtyka O, Kubicki J, et al. Biodiesel production on MgO, CaO, SrO and BaO oxides supported on (SrO)(Al₂O₃) mixed oxide. *Catal Lett* 2015;145:1196–205.
- Ramkumar S, Kirubakaran V. Biodiesel from vegetable oil as alternate fuel for C.I engine and feasibility study of thermal cracking: a critical review. *Energy Convers Manage* 2016;118:155–69.
- Nalgundwar A, Paul B, Sharma SK. Comparison of performance and emissions characteristics of DI CI engine fueled with dual biodiesel blends of palm and jatropha. *Fuel* 2016;173:172–9.
- Yang L, Lv P, Yuan Z, Luo W, Li H, Wang Z, et al. Synthesis of biodiesel by different carriers supported KOH catalyst. *Adv Mater Res* 2012:197–201.
- da Costa Evangelista JP, Gondim AD, Souza LD, Araujo AS. Alumina-supported potassium compounds as heterogeneous catalysts for biodiesel production: a review. *Renew Sustain Energy Rev* 2016;59:887–94.
- Senthil M, Visagavel K, Saravanan CG, Rajendran K. Investigations of red mud as a catalyst in Mahua oil biodiesel production and its engine performance. *Fuel Process Technol* 2016;149:7–14.
- Qu L, Wang Z, Zhang J. Influence of waste cooking oil biodiesel on oxidation reactivity and nanostructure of particulate matter from diesel engine. *Fuel* 2016;181:389–95.
- Benessere V, Cucciolo ME, Esposito R, Lega M, Turco R, Ruffo F, et al. A novel and robust homogeneous supported catalyst for biodiesel production. *Fuel* 2016;171:1–4.
- Farooq M, Ramli A, Subbarao D. Biodiesel production from waste cooking oil using bifunctional heterogeneous solid catalysts. *J Cleaner Prod* 2013;59:131–40.
- Kim M, DiMaggio C, Salley SO, Simon Ng KY. A new generation of zirconia supported metal oxide catalysts for converting low grade renewable feedstocks to biodiesel. *Bioresour Technol* 2012;118:37–42.
- Tamborini LH, Casco ME, Militello MP, Silvestre-Albero J, Barbero CA, Acevedo DF. Sulfonated porous carbon catalysts for biodiesel production: clear effect of the carbon particle size on the catalyst synthesis and properties. *Fuel Process Technol* 2016;149:209–17.
- Muciu GEG, Romero R, García-Orozco I, Serrano AR, Jiménez RB, Natividad R. Deactivation study of K₂O/NaX and Na₂O/NaX catalysts for biodiesel production. *Catal Today* 2016;271:220–6.
- Istadi I, Anggoro DD, Buchori L, Rahmawati DA, Intaningrum D. Active acid catalyst of sulphated zinc oxide for transesterification of soybean oil with methanol to biodiesel. *Proc Environ Sci* 2015;23:385–93.
- Jaya N, Selvan BK, Vennison SJ. Synthesis of biodiesel from pongamia oil using heterogeneous ion-exchange resin catalyst. *Ecotoxicol Environ Saf* 2015;121:3–9.
- Hernández-Hipólito P, Juárez-Flores N, Martínez-Klimova E, Gómez-Cortés A, Bokhimi X, Escobar-Alarcón L, et al. Novel heterogeneous basic catalysts for biodiesel production: sodium titanate nanotubes doped with potassium. *Catal Today* 2015;250:187–96.
- Zhou Q, Zhang H, Chang F, Li H, Pan H, Xue W, et al. Nano La₂O₃ as a heterogeneous catalyst for biodiesel synthesis by transesterification of *Jatropha curcas* L. oil. *J Ind Eng Chem* 2015;31:385–92.
- Soltani S, Rashid U, Yunus R, Taufiq-Yap YH. Biodiesel production in the presence of sulfonated mesoporous ZnAl₂O₄ catalyst via esterification of palm fatty acid distillate (PFAD). *Fuel* 2016;178:253–62.
- Islam A, Taufiq-Yap YH, Chu C-M, Chan E-S, Ravindra P. Studies on design of heterogeneous catalysts for biodiesel production. *Process Saf Environ Prot* 2013;91:131–44.
- Cirujano FG, Corma A, Labrés i Xamena FX. Zirconium-containing metal organic frameworks as solid acid catalysts for the esterification of free fatty acids: synthesis of biodiesel and other compounds of interest. *Catal Today* 2015;257(Part 2):213–20.
- Muthu H, SathyaSelvabala V, Varathachary TK, Kirupha Selvaraj D, Nandagopal J, Subramanian S. Synthesis of biodiesel from neem oil using sulfated zirconia via transesterification. *Braz J Chem Eng* 2010;27:601–8.
- Brito A, Borges ME, Garin M, Hernández A. Biodiesel production from waste oil using Mg–Al layered double hydroxide catalysts. *Energy Fuels* 2009;23:2952–8.
- Čapek L, Kutálek P, Smoláková L, Hájek M, Troppová I, Kubička D. The effect of thermal pre-treatment on structure, composition, basicity and catalytic activity of Mg/Al mixed oxides. *Top Catal* 2013;56:586–93.
- Prado RG, De Almeida GD, De MM, Carvalho O, Galvão LM, Bejan CCC, et al. Multivariate method for transesterification reaction of soybean oil using calcined Mg–Al layered double hydroxide as catalyst. *Catal Lett* 2014;144:1062–73.

- [28] Hájek M, Kutálek P, Smoláková L, Troppová I, Čapek L, Kubička D, et al. Transesterification of rapeseed oil by Mg–Al mixed oxides with various Mg/Al molar ratio. *Chem Eng J* 2015;263:160–7.
- [29] Wang Y, Zhang F, Xu S, Yang L, Li D, Evans DG, et al. Preparation of macrospherical magnesia-rich magnesium aluminate spinel catalysts for methanolysis of soybean oil. *Chem Eng Sci* 2008;63:4306–12.
- [30] Hassani Rad SJ, Haghghi M, Alizadeh Eslami A, Rahmani F, Rahemi N. Sol-Gel vs. impregnation preparation of MgO and CeO₂ doped Ni/Al₂O₃ nanocatalysts used in dry reforming of methane: effect of process conditions, synthesis method and support composition. *Int J Hydrogen Energy* 2016;41:5335–50.
- [31] Yahyavi SR, Haghghi M, Shafiei S, Abdollahifar M, Rahmani F. Ultrasound-assisted synthesis and physicochemical characterization of Ni-Co/Al₂O₃-MgO nanocatalysts enhanced by different amounts of MgO used for CH₄/CO₂ reforming. *Energy Convers Manage* 2015;97:273–81.
- [32] Schmidtmeier Dagmar, Büchel Gunter, Buhr A. Magnesium aluminate spinel raw materials for high performance refractories for steel ladles. *Ceram Mater* 2009;61:223–7.
- [33] Sajjadi SM, Haghghi M, Rahmani F. Syngas production from CO₂-reforming of CH₄ over sol-gel synthesized Ni-Co/Al₂O₃-MgO-ZrO₂ nanocatalyst: effect of ZrO₂ precursor on catalyst properties and performance. *Quim Nova* 2015;38:459–65.
- [34] Sajjadi SM, Haghghi M, Rahmani F. Sol-gel synthesis and catalytic performance of Ni-Co/Al₂O₃-MgO-ZrO₂ nanocatalyst with different ZrO₂ loadings used in CH₄/CO₂ reforming for hydrogen production. *Int J Oil, Gas Coal Technol* 2014;8:304–24.
- [35] Abdollahifar M, Haghghi M, Babaluo AA, Talkhoncheg S Khajeh. Sono-synthesis and characterization of bimetallic Ni-Co/Al₂O₃-MgO nanocatalyst: effects of metal content on catalytic properties and activity for hydrogen production via CO₂ reforming of CH₄. *Ultrason Sonochem* 2016;31:173–83.
- [36] Sajjadi SM, Haghghi M, Rahmani F. Dry reforming of greenhouse gases CH₄/CO₂ over MgO-promoted Ni-Co/Al₂O₃-ZrO₂ nanocatalyst: effect of MgO addition via sol-gel method on catalytic properties and hydrogen yield. *J Sol-Gel Sci Technol* 2014;70:111–24.
- [37] Allahyari S, Haghghi M, Ebadi A, Hosseinzadeh S. Effect of irradiation power and time on ultrasound assisted co-precipitation of nanostructured CuO-ZnO-Al₂O₃ over HZSM-5 used for direct conversion of syngas to DME as a green fuel. *Energy Convers Manage* 2014;83:212–22.
- [38] Khoshbin R, Haghghi M. Urea-nitrate combustion synthesis and physicochemical characterization of CuO-ZnO-Al₂O₃ nanoparticles over HZSM-5. *Chin J Inorg Chem* 2012;28:1967–78.
- [39] Scherrer P. Bestimmung der Größe und der inneren Struktur von Kolloidteilchen mittels Röntgenstrahlen. *Nachrichten von der Gesellschaft der Wissenschaften zu Göttingen* 1918;26:98–100.
- [40] Aruna ST, Rajam KS. Mixture of fuels approach for the solution combustion synthesis of Al₂O₃-ZrO₂ nanocomposite. *Mater Res Bull* 2004;39:157–67.
- [41] Li F-T, Zhao Y, Liu Y, Hao Y-J, Liu R-H, Zhao D-S. Solution combustion synthesis and visible light-induced photocatalytic activity of mixed amorphous and crystalline MgAl₂O₄ nanopowders. *Chem Eng J* 2011;173:750–9.
- [42] Coenen JWE. Catalytic hydrogenation of fatty oils. *Ind Eng Chem Fundam* 1986;25:43–52.
- [43] Granados ML, Poves MDZ, Alonso DM, Mariscal R, Galisteo FC, Moreno-Tost R, et al. Biodiesel from sunflower oil by using activated calcium oxide. *Appl Catal B* 2007;73:317–26.
- [44] Abramoff MD, Magalhaes PJ, Ram SJ. Image processing with ImageJ. *Biophotonics Int* 2004;11:36–42.
- [45] Chorghand M, Haghghi M, Saedy S, Aghamohammadi S. Efficient hydrothermal synthesis of nanostructured SAPO-34 using ultrasound energy: physicochemical characterization and catalytic performance toward methanol conversion to light olefins. *Adv Powder Technol* 2014;25:1728–36.
- [46] Parvas M, Haghghi M, Allahyari S. Degradation of phenol via wet-air oxidation over CuO/CeO₂-ZrO₂ nanocatalyst synthesized employing ultrasound energy: physicochemical characterization and catalytic performance. *Environ Technol* 2014;35:1140–9.
- [47] Estifae P, Haghghi M, Babaluo AA, Rahemi N, Jafari M Fallah. The beneficial use of non-thermal plasma in synthesis of Ni/Al₂O₃-MgO nanocatalyst used in hydrogen production from reforming of CH₄/CO₂ greenhouse gases. *J Power Sources* 2014;257:364–73.
- [48] Abbasi Z, Haghghi M, Fatehifar E, Saedy S. Synthesis and physicochemical characterization of nanostructured Pt/CeO₂ catalyst used for total oxidation of toluene. *Int J Chem Reactor Eng* 2011;9:1–19.
- [49] Navaei Alvar E, Rezaei M, Navaei Alvar H, Feyzallahzadeh H, Yan Z-F. Synthesis of nanocrystalline MgAl₂O₄ spinel by using ethylene diamine as precipitation agent. *Chem Eng Commun* 2009;196:1417–24.
- [50] Saberi A, Golestani-Fard F, Sarpoolaky H, Willert-Porada M, Gerdes T, Simon R. Chemical synthesis of nanocrystalline magnesium aluminate spinel via nitrate-citrate combustion route. *J Alloy Compd* 2008;462:142–6.
- [51] Taibi M, Ammar S, Jouini N, Fievet F, Molinie P, Drillon M. Layered nickel hydroxide salts: synthesis, characterization and magnetic behaviour in relation to the basal spacing. *J Mater Chem* 2002;12:3238–44.
- [52] Li L-X, Xu D, Li X-Q, Liu W-C, Jia Y. Excellent fluoride removal properties of porous hollow MgO microspheres. *New J Chem* 2014;38:5445–52.
- [53] Momeni SM, Pakizeh M. Preparation, characterization and gas permeation study of PSf/MgO nanocomposite membrane. *Braz J Chem Eng* 2013;30:589–97.
- [54] Silva CCCM, Ribeiro NFP, Souza MMVM, Aranda DAG. Biodiesel production from soybean oil and methanol using hydrotalcites as catalyst. *Fuel Process Technol* 2010;91:205–10.
- [55] Kutálek P, Čapek L, Smoláková L, Kubička D. Aspects of Mg–Al mixed oxide activity in transesterification of rapeseed oil in a fixed-bed reactor. *Fuel Process Technol* 2014;122:176–81.
- [56] Barakos N, Pasiás S, Papayannakos N. Transesterification of triglycerides in high and low quality oil feeds over an HT2 hydrotalcite catalyst. *Bioresour Technol* 2008;99:5037–42.